Structure-based analysis of boronic acids as inhibitors of Acinetobacter-derived cephalosporinase-7 (ADC-7), a unique class C β-lactamase

Journal:	*ACS Infectious Diseases*
Manuscript ID	id-2017-001524.R1
Manuscript Type:	Article
Date Submitted by the Author:	n/a
Complete List of Authors:	Bouza, Alexandra; Grand Valley State University, Chemistry Swanson, Hollister; Grand Valley State University, Chemistry Smolen, Kali; Grand Valley State University, Chemistry VanDine, Alison; Grand Valley State University, Chemistry Taracila, Magdalena; Louis Stokes Cleveland Department of Veterans Affairs Medical Center, Research Service; Case Western Reserve University School of Medicine ROMAGNOLI, CHIARA; University of Modena and Reggio Emilia, Department of Life Sciences Caselli, Emilia ; University of Modena and Reggio Emilia, Department of Life Sciences Prati, Fabio; University of Modena and Reggio Emilia, Department of Life Sciences Bonomo, Robert; Louis Stokes Veterans Administration Medical Center, Infectious Diseases; Case Western Reserve University School of Medicine Powers, Rachel; Grand Valley State University, Chemistry Wallar, Bradley; Grand Valley State University, Chemistry

Structure-based analysis of boronic acids as inhibitors of Acinetobacter-derived cephalosporinase-7 (ADC-7), a unique class C β-lactamase

Alexandra A. Bouza[1#], Hollister C. Swanson[1#], Kali A. Smolen[1], Alison L. VanDine[1], Magdalena A. Taracila[3,4], Chiara Romagnoli[2], Emilia Caselli[2], Fabio Prati[2], Robert A. Bonomo[3,4*], Rachel A. Powers[1*], and Bradley J. Wallar[1*]

[1] Department of Chemistry, 1 Campus Drive, Grand Valley State University, Allendale, MI, 49401

[2] Department of Life Sciences, University of Modena and Reggio Emilia, Via Campi 103, 41125 Modena, Italy

[3] Research Service, Louis Stokes Cleveland Department of Veterans Affairs Medical Center, 10701 East Boulevard, Cleveland, OH 44106

[4] Departments of Medicine, Pharmacology, Molecular Biology and Microbiology, Case Western Reserve University School of Medicine Cleveland, OH 44106

* Corresponding authors, Robert.bonomo@va.gov; powersra@gvsu.edu; wallarb@gvsu.edu

\# These authors contributed equally to the manuscript

Acinetobacter baumannii is a multidrug resistant pathogen that infects more than 12,000 patients each year in the US. Much of the resistance to β-lactam antibiotics in *Acinetobacter spp.* is mediated by class C β-lactamases known as *Acinetobacter*-derived cephalosporinases (ADCs). ADCs are unaffected by clinically used β-lactam-based β-lactamase inhibitors. In this study, five boronic acid transition state analog inhibitors (BATSIs) were evaluated for inhibition of the class C cephalosporinase ADC-7. Our goal was to explore the properties of BATSIs designed to probe the R1 binding site. K_i values ranged from low micromolar to sub-nanomolar, and circular dichroism (CD) demonstrated that each inhibitor stabilizes the β-lactamase-inhibitor complexes. Additionally, X-ray crystal structures of ADC-7 in complex with five inhibitors were determined (resolutions from 1.80-2.09 Å). In the ADC-7/CR192 complex, the BATSI with the lowest K_i (0.45 nM) and greatest ΔTm (+9 °C), a trifluoromethyl substituent interacts with Arg340. Arg340 is unique to ADCs and may play an important role in the inhibition of ADC-7. The ADC-7/BATSI complexes determined in this study shed light into the unique recognition sites in ADC enzymes, and also offer insight into further structure-based optimization of these inhibitors.

Keywords: β-lactamase, cephalosporinase, boronic acid, transition state analog inhibitors, *Acinetobacter,* ADC-7

Since the discovery of penicillin in the late 1920s, antibiotic resistance has been a major threat to human health.[1] During the past decade, resistance to all classes of β-lactam antibiotics (penicillins, cephalosporins, carbapenems) among *Acinetobacter baumannii* has considerably increased.[2-6] Although there are many mechanisms that contribute to the resistance, such as efflux pumps and porins, β-lactamases are the primary cause of resistance to β-lactam antimicrobials.[1]

β-lactamases function by hydrolyzing the amide bond in the lactam ring of β-lactam antibiotics, preventing β-lactam inhibition of its original cellular targets the transpeptidases.[2, 7] A significant portion of the β-lactamase-mediated resistance in *Acinetobacter* results from a unique family of class C enzymes, the *Acinetobacter*-derived cephalosporinases (ADCs).[2, 8-9] ADCs are chromosomally encoded β-lactamases responsible for resistance to cephalosporin antibiotics such as cephalexin.[8] Specifically, ADC-7 was identified in a clinical isolate of *A. baumannii* that exhibited extended-spectrum activity against numerous β-lactams.[8] In addition, ADCs are unique from other class C β-lactamases as they possess several distinct active site residues.[10] These evolutionarily induced sequence differences in ADC-7 serve as a potential explanation for the enzyme's plasticity in catalyzing multiple cephalosporins and may aid in targeted drug discovery efforts.[11]

One way to circumvent β-lactamase-mediated resistance is using β-lactamase inhibitors (BLIs) **(Figure 1)**. Current commercially available BLIs, like sulbactam and clavulanic acid, are prescribed in combination therapies with a partner β-lactam antibotic.[11] Unfortunately, these BLIs are themselves β-lactams, and bacteria are able to develop resistance rapidly against these chemically similar molecules.[12] Moreover, these BLIs have been shown to be ineffective against *Acinetobacter spp.*, with relatively high K_i values (500-4,000 μM) for clinically used BLIs.[8] The

design of novel BLIs is essential to overcome cephalosporinase-mediated resistance in *Acinetobacter* and its overwhelming clinical threat.[13]

Novel non-β-lactam-based BLIs have been identified and characterized, including the phosphonates[14], hydroxamates[15], and diazabicyclooctanes (DBOs).[16-17] In 2015, the FDA approved the combination therapy known as Avycaz,™ which pairs the third-generation cephalosporin ceftazidime with the novel DBO inhibitor avibactam.[18] Another class of novel BLIs are the boronic acids, transition state analog inhibitors (BATSIs) that have long been known to inhibit class A and C β-lactamases **(Figure 1)**.[10, 19-20, 12] Previous work in our group suggested that BATSIs offer excellent potential as inhibitors of ADC enzymes in *A. baumannii*, specifically ADC-7, with K_i values in the nanomolar range.[10] Additionally, the X-ray crystal structure of ADC-7 in complex with the BATSI S02030 (PDB 4U0X[10]) provided insight into ways this series might be optimized.

In the present study, a select group of five different BATSIs (4 from the CR series and 1 from the S series) were characterized via X-ray crystallography and kinetic analysis and shown to bind with high affinity and inhibit ADC-7 activity. These BATSIs were chosen due to their effectiveness in microbiological disc susceptibility assays, as well as their ability to probe interactions between active site residues and the R1 inhibitor group, which is meant to resemble the R1 side chains of β-lactam antibiotics **(Fig. 1A, C)**. Canonical binding sites identified in related class C β-lactamase/BATSI complexes were also observed in these ADC-7 complexes. However, several unique interactions and binding sites were identified in these newly determined structures. One such binding site is comprised of Asn213 and Ser317 and serves to bind the distal carboxylate and/or tetrazole groups in common to the CR inhibitor series. The optimization of these BATSIs will aid in mapping the ADC-7 active site for inhibitor "hot spot" binding sites

and contribute to our understanding of β-lactamase mediated antibiotic resistance in *Acinetobacter*.

RESULTS AND DISCUSSION

Microbiology, Thermal Stability, and Kinetics

In order to assess the potency of the inhibitors in whole cells, MIC and disc susceptibility assays were performed using *E. coli* DH10B expressing *wt*ADC-7 and the R340A variant. When the compounds were paired with the β-lactam ceftazidime (10 μg CAZ and 10 μg BATSI), the disk zone sizes increased from 12 mm for CAZ alone to 20-26 mm for all the compounds in the CR series (**Table 1A**). When the sulfonamide group present in the CR series compounds is replaced by triazole (S series compound S06017), the zone size decreased to 15 mm. A similar trend was observed when MICs were performed. Using a fixed concentration of the BATSIs (4 μg/mL) and varying CAZ concentrations, the MIC values were shown to decrease from 64 μg/mL to lower than 2 μg/mL (0.5 μg/mL for CR161, 1 μg/mL for CR167 and CR157, and 2 μg/mL for CR192) (**Table 1B**). Consistent with the trend of the DSA studies, the MIC for S06017 was much higher (16 μg/mL) than compounds in the CR series. In the MDR clinical strain, from which ADC-7 was initially cloned, we also see a reduction of MIC values from > 64 to 8 μg/mL for the CR series and 16 μg/mL to S06017. The reduction of MICs to 8 μg/mL is most encouraging as the lack of permeability across the outer membrane of *A. baumannii* is a significant challenge in medicinal chemistry.[10] Interestingly, the mutation at the distal site Asn213Ala, preserved the MICs for most of the compounds. The interactions between the tetrazole and backbone atoms of the Ala residue are probably preserved and/or interactions with Ser317 compensate for the loss of Asn213 interactions. The MIC for CR192 in *E. coli* decreased

from 2 μg/mL to 1 μg/mL for the Asn213Ala variant. Similar behavior was observed for CR192 with the Arg340Ala ADC-7 variant, but the MIC decrease is larger, 0.5 μg/mL. The Lys variant restored the MIC of the wild type. This may suggest that the tetrazole interactions with the distal site Asn213/Ser317 are more beneficial in terms of preserving the affinity and potency of the inhibitors when the mutations in the active site of the enzyme occur. With respect to position 340, the MICs for CR161 and CR157 do not change significantly with the mutations.

We observed that the thermal stability of the ADC-7 enzyme increases when complexed with BATSI (**Figure 2**). The variation in melting temperature are from 2°C for S06017 and CR161, to 4°C for CR157 and CR161 complexes. The larger variation is for CR192: ADC-7 complex, which increases the T_m by 9°C (**Table 2**). The R340A and N213A mutations do not change the thermal stability of the enzyme, preserving the melting temperature of $T_m \approx$ 61-62°C.

The binding affinity of ADC-7 for the five BATSIs was assessed using competition kinetics. The initial velocities were determined by utilizing NCF as a colorimetric indicator substrate. As shown in **Table 2**, all the BATSIs tested were effective inhibitors of ADC-7, with one K_i value, CR192, dropping into the sub-nanomolar range. The weakest binding BATSI, S06017, had a K_i of 6.11 μM. While each of the CR inhibitors bound to ADC-7 with high affinity, the best inhibitor was CR192, which had a K_i of 0.45 nM. The weakest binding BATSI in the CR series was CR167, which still had a relatively low K_i of 160 nM. The remaining two CR BATSIs tested, CR161 and CR157, possessed K_i values of 7.8 and 38 nM, respectively.

X-ray crystal structure of ADC-7/inhibitor complexes

Structure Determination

To characterize the specific active site interactions with the inhibitors, all five ADC-7/BATSI complexes were determined via X-ray crystallography. The CR167, CR157, CR161,

CR192, and S06017 complexes were determined to 1.80, 2.06, 2.09, 2.03, and 1.93 Å respectively. Each ADC-7/BATSI complex crystallized in the $P2_1$ space group with four monomers in the asymmetric unit (**Table 3**). The structure was determined via molecular replacement using the ADC-7 structure from *A. baumannii* (PDB 4u0t) with waters and ions removed.[10] Inspection of the initial F_o-F_c electron density maps contoured at 3σ demonstrated that each inhibitor was bound in the active sites of all four monomers comprising the asymmetric unit. For all structures, electron density for the inhibitors was contiguous with the Oγ atom of Ser64, indicative of the expected covalent attachment with the boron of the inhibitors (**Figure 3**). F_o-F_c omit maps contoured at 3.0 σ confirmed the presence of each inhibitor, their covalent attachments to Ser64, and the tetrahedral geometry about the boron which mimics the presumed transition state in β-lactam hydrolysis. Unexpectedly, electron density maps of all five ADC-7/BATSI complexes revealed that the boronic acid O2 atom was modified with the addition of a covalently bound phosphate ion **(Figure 3)**. Superposition of the four monomers of the asymmetric unit in each of the ADC-7/BATSI crystal structure shows that the inhibitor binds in nearly identical orientations in each site, with mean RMSDs for superposition of all inhibitor atoms ranging from 0.8 Å for the CR157 complex, 0.5 Å for CR161, 0.6 Å for CR167 and S06017, and 0.7 Å for CR192. In all cases, thermal B factors are lowest for the B monomer. For simplicity, the B monomer is used as representative of all monomers.

Canonical Interactions

As expected, in every structure, the O1 hydroxyl groups of the BATSIs are bound in the oxyanion hole, hydrogen bonding with the main chain nitrogens of Ser64 and Ser315 and the main chain oxygen of Ser315 **(Figure 4)**. The boronic acid O2 hydroxyl group is usually observed to form hydrogen bonds with Tyr150OH and a well-ordered water molecule, believed

to represent the deacylating water. The interaction between the O2 and Tyr150 is maintained in the CR series of BATSIs but not in the S06017 structure. That this interaction is still present in the CR series is somewhat surprising, given that the boronic acid O2 group has been covalently modified with a phosphate group. In the CR structures, the phosphate forms hydrogen bonds with approximately two or three water molecules as well as the hydroxyl group of Thr313. In the S06017 structure, the phosphate group is oriented to form hydrogen bonds with Tyr150. The presumed deacylating water is present in each structure, except it interacts with one of the phosphate oxygens, not the O2 hydroxyl.

The CR series of inhibitors replace the R1 amide found in the R1 side chains of β-lactams with a sulfonamide group. In the crystal structures, one of the sulfonyl oxygens mimics the amide oxygen by hydrogen bonding with the side chain amide nitrogens of Gln120 and Asn152 **(Figure 5)**.[21] However, the sulfonamide nitrogen does not hydrogen bond to the main chain carbonyl oxygen of Ser315, as the R1 amide nitrogen does in complexes with β-lactams.

Variable Interactions

Beyond the canonical interactions maintained with the core boronic acid group of the BATSIs, each of the inhibitors display interactions with the enzyme that are unique to their R1 groups. In contrast to the sulfonamide found in the R1 groups of the CR series, S06017 contains a triazole ring. Similar to the sulfonamide, the triazole ring also hydrogen bonds to the side chain amide nitrogens of both Gln120 and Asn152 (3.0-3.2 Å).

Following the sulfonamide, the CR series all contain a conjugated aryl ring in the R1 group of the inhibitors. The aryl rings of CR157, CR161, and CR192 all form edge-to-face π-π stacking interactions with Tyr222. The aryl ring of CR167 also interacts with Tyr222 although the interaction with this residue is a parallel displaced π-π stacking interaction **(Figure 7)**.

The distal ends of the R1 groups of each of the BATSIs contain a negatively charged group, either a carboxylate (CR167, S06017) or a tetrazole group (CR157, CR161, CR192). The distal functional group of CR157, CR161, CR167 and CR192 all bind in a site formed by Asn213 and Ser317 at the edge of the active site. The carboxylate/tetrazole groups form favorable hydrogen bonding interactions (between 2.8-3.2 Å) with the main chain nitrogen atoms of Asn213 and Ser317. A hydrogen bond is also formed between the tetrazole/carboxylate of CR157, CR192, and CR167 and the side chain Oγ of Ser317 (~3.2 Å). The anionic tetrazole/carboxylate groups also make hydrogen bonds with either one (CR157 and CR167) or two (CR161 and CR192) water molecules **(Figure 5)**. Due to its shorter R1 group, the carboxylate of S06017 is unable to reach the distal Asn213/Ser317 site. Instead, the S06017 carboxylate makes ionic interactions with Arg340 (2.8-3.1 Å). Unique to CR192, a distinct interaction between the trifluoromethyl group of the inhibitor and the side chain of Arg340 is observed (4.0 Å; **Figure 6**).

A combination of several functional assays with the X-ray crystal structures of five different ADC-7/BATSI complexes revealed important insight for targeting favorable interactions with the R1 binding site of ADC-7 cephalosporinase. Analysis of key interactions observed in the structures support the inhibition data obtained through kinetic studies.

Unexpectedly, in all the ADC-7/BATSI complexes, F_o-F_c difference electron density maps revealed a significant (> 3 σ) peak that appeared to be covalently bonded with the O2 of the boronic acid. A phosphate group was modeled into these peaks, and the final structures support phosphorylation of the boronic acid O2 hydroxyl groups **(Figure 3)**. The covalently attached phosphate is observed in all five of the ADC-7/BATSIs complexes presented here. However, this modification was not observed in the structure of our first ADC-7/BATSI complex

(PDB 4U0X; **Figure 3)**.[10] The main difference between the previously determined ADC-7/BATSI complex (S02030) and the ones presented here is that the original inhibitor also contained an R2 group (**Figure 1C**).[10] The CR series BATSIs from this study do not possess an R2 group. The presence of the R2 group may prevent phosphorylation of the O2 hydroxyl by occluding access to this functional group. The O2 phosphorylation may be a crystallographic artifact stemming from the phosphate buffer used in crystallization, as a phosphate ion is observed bound in the active site of the apoADC-7 structure.[10] However, O2 phosphorylation is not observed in studies with the related class C β-lactamase AmpC in complexes with four of the same inhibitors bound, and AmpC also crystallizes in phosphate buffer, although at a higher pH (pH 8.6-8.8 vs. pH 5 for ADC-7).[19]

An important feature in the design of the R1 BATSIs is their ability to mimic the R1 amide found in β-lactam antibiotics, as well as the previously studied BATSI S02030. In both the ADC-7/S02030 complex[10] and in the AmpC/cephalothin complex[21], the amide group forms hydrogen bonds with the side chains of Gln120 and Asn152, as well as the main chain carbonyl oxygen of Ser315. In this study, four of the BATSIs replace the amide with a sulfonamide **(Table 2)**. The X-ray crystal structures revealed that the sulfonamide formed hydrogen bonds in a similar fashion to Gln120 and Asn152, although it lacks the hydrogen bond with the main chain of Ser315 **(Figures 4, 5)**. Notably, the K_i values for all CR BATSIs are in the nM range; these observations demonstrate that a sulfonamide is a successful, although not perfect, mimic of the β-lactam R1 amide group.[10] The mode of binding to the sulfonamide was consistent with AmpC/CR167, in which both Gln120 and Asn152 interacted with the sulfonamide; however, the AmpC complexes with CR157, CR161, and CR192 showed Gln120 side chain adopting a conformation swung out from the active site so that it no longer interact with sulfonamides of

these BATSIs.[19] Alternatively, S06017 was designed to contain a triazole group in place of the R1 amide/sulfonamide. The triazole group, a known non-classical amide bioisoster easily accessible by click-chemistry reaction, provides a chemical moiety from which numerous combinations of compounds can be engineered with relatively efficient synthesis.[22] Indeed, the triazole forms hydrogen bonds with the conserved Gln120 and Asn152 residues, but not Ser315, seemingly to work as a mimic for the sulfonamide **(Figure 4)**. However, microbiological studies indicated that this BATSI was the least efficient inhibitor, as it had the highest MIC and lowest DSA value for any of the five tested BATSIs (**Table 1**). In addition, kinetic studies revealed that S06017 exhibits the lowest binding affinity to ADC-7 (K_i = 6.1 μM) indicating that certain structural features are lacking in S06017, providing few interactions in the active site, thereby accounting for the overall poor binding affinity.

In the previous study of ADC-7 with S02030, a potential distal carboxylate binding site adjacent to the R1 group was proposed, with potential binding partners of Gln120 and Ser317.[10] In this study, each of the BATSIs contained either an extended R1 group terminating in a carboxylate or tetrazole, substituents that contain similar electronic and steric features. As proposed, the terminal substituent of all four CR BATSIs formed hydrogen bonds with the backbone atoms of Ser317 and Asn213, resulting in low K_i values for these inhibitors (**Figure 4A-D**). In the microbiological studies of the CR BATSIs, the Asn213Ala mutation causes a 2- to 4-fold increase in the MIC values. While the Asn213 interaction is via the main chain, it is possible that the change in side chain moves the backbone atoms enough to decrease H-bonding with the R1 carboxylate/tetrazole. The fifth BATSI, S06017, is distinguished by a shorter R1 group, and the carboxylate group is unable to reach the distal site to form interactions with Asn213 and Ser317 (**Figure 4E)**. Instead, the carboxylate forms an ionic bond with the side

chain of Arg340. However, even with the addition of this interaction with Arg340, as stated earlier, the S06017 has the lowest binding affinity to ADC-7. This would suggest that the ADC-7/BATSI interactions involving the distal active site residues, Ser317 and Asn213, serve to play a role in binding the inhibitor in ADC-7. Sequence alignment among ADC enzymes shows that Asn213 is completely conserved, whereas position 317 consists of either serine (ADC-7), asparagine, or threonine; all of which have the potential to form interactions with the inhibitor via main chain and side chain hydrogen bonds.

The active site Arg340 is unique to the ADC enzymes among class C β-lactamases. While it has been previously shown to interact with the R2 carboxylate of S02030 [10], as well as with the R1 carboxylate of S06017, it does show an interesting interaction with the CR192 BATSI. The only structural difference between the two inhibitors, CR157 and CR192, is the trifluoromethyl substituent on the phenyl ring of CR192, which resulted in a significant (almost 100-fold) increase in affinity for ADC-7 **(Table 2, Figure 6)**. Both complexes have identical active site interactions, except the trifluoromethyl substituent on CR192 interacts with Arg340. This specific interaction has the potential to be either a coulombic interaction or a hydrogen bond with the Arg340 acting as the donor and the fluorines acting as acceptors. Analysis of the interaction in all four monomers suggests that the center of the trifluoromethyl points at the carbon of the guanidinium group of Arg340. These two centers are within ionic bond distance (4.0 Å) and could be a coulombic interaction with the fluorines partial negative charges summing to a net negative charge.[23-25] Regardless of whether it is involved in hydrogen bond or coulombic interactions, the arginine is oriented at an angle toward the side of the C-F bonds which is consistent with more negative electron potential being located on the side of the fluorines in the C-F bonds.[26] Whether the interaction is hydrogen bonding or columbic, the

structural data combined with kinetic studies reveal this interaction provides increased affinity down to the low nanomolar range **(Table 2)**. In addition, the K_i was determined for the ADC-7/R340A mutant with CR192 (8.3 nM). This is ~ 20-fold weaker binding to CR192 than wild type ADC-7 (K_i of 0.45 nM), confirming the contribution of the R340 interaction to the overall binding affinity to CR192. Conversely, in a complex that lacks any interaction with R340 (ADC-7/CR161), the R340A mutation does not cause a significant decrease in the binding affinity to CR161 (K_i of 2.1 nM vs. 7.8 nM for wild type ADC-7/CR161).

Microbiological studies indicate that the Arg340Ala does not affect the MIC for CR157, CR167, and CR161, which is consistent with the X-ray structural data showing that Arg340 does not interact with those BATSIs. The "anchoring "effect of the distal site interactions with BATSI is more relevant for the CR192 compound. The Arg340 mutation (**Table 1B**), with the loss of the Arg340/CR192 trifluoromethyl interaction, does not result in an increase in MIC, suggesting that the distal site interaction is preserved (the MIC decreases from 2 to 0.5 μg/mL). Despite knowing that the Arg340Ala mutation lowers the binding affinity to CR192, ADC-7_{R340A} retains an overall tight binding affinity that does not appear to negatively impact the MIC results.

Finally, another interaction between ADC-7 and the CR BATSIs that may contribute to the binding, as well as explain some of the differences in binding affinity, is the aryl interaction with Tyr222 and the aromatic rings of the inhibitors. Consistent with the interactions with these BATSIs and the analogous residue of AmpC (Tyr221)[19], the phenyl rings of CR157, CR161, and CR192 form edge-to-face π-π stacking at angles of 63°, 57°, 58° respectively, while the benzyl ring of CR167 forms parallel displaced π-π stacking at an angle of 18° (**Figure 7**).[27-28] A potential reason for the different π-π conformation may be a result of the extra carbon linker observed in CR167, allowing an extra degree of rotational freedom. CR167 possesses a K_i of 160

nM, a minimum of four-fold larger than the other K_i values, suggesting that edge-to-face π-π stacking may provide a higher affinity than parallel displaced, though this may also be attributed to other small differences in active site interactions. The structures of CR157, CR161, and CR192 are strikingly similar; yet, the inhibitors have varying affinities for ADC-7. Analysis of the X-ray crystal structures of these complexes cannot fully explain why replacing the aryl ring of CR157 with a pyridine ring in CR161 results in a 5-fold greater affinity for ADC-7. One potential reason is that with the pyridine nitrogen pointing away from the Tyr222 aryl ring (CR161), the hydrogens on the opposite side of the pyridine ring have been shown to be more effective "π-hydrogen bond donors" as compared to phenyl ring lacking a heteroatom (CR157).[29]

Overall, this study provides insight into inhibitor recognition and design for ADC β-lactamases. Comparing the inhibitors, it is clear that optimizing an inhibitor for ADC-7 will include forming interactions with the distal carboxylate binding site, comprised of residues Asn213 and Ser317. From the kinetic studies, the edge-to-face π-π stacking is optimal for greater affinity. Observing the unique interaction between the trifluoromethyl and Arg340, forming interactions with this residue provides higher affinity for ADC-7. Resulting from the previous ADC-7/S02030 complex and CR192 complex, the plasticity for varying interactions with Arg340 are possible. Further exploration into Arg340 interactions will be beneficial in further optimization of BATSIs.

METHODS

Synthesis and Chemical Analysis

CR157, CR161, CR167, and CR192 were synthesized as previously described.[19] The synthesis of S06017 was also previously described.[22]

Disc Susceptibility Assays (DSAs) and Minimum Inhibitory Concentrations (MICs)

DSAs and MICs were performed as previously described,[10] and according to Clinical and Laboratory Standards Institute (CLSI) guidelines.[30] Bacterial cultures were grown overnight in Mueller-Hinton (MH) broth supplemented with 20 μg/mL of chloramphenicol to ensure maintenance of the β-lactamase plasmid in pBC SK (−) containing *Escherichia coli* strains. Liquid culture was then diluted using MH broth to a McFarland Standard (OD_{600} = 0.224). Bacteria were plated on MH agar and a disc containing 10 μg of compound and 10 μg of ceftazidime was added. After an overnight incubation at 37 °C, zone sizes were measured and reported.

Susceptibility profiles (MIC's) were determined by cation-adjusted MH agar dilution and liquid microdilution. We employed the *E. coli* construct in a uniform genetic background (blaADC‑7 was directionally cloned in pBC SK (−) phagemid vector under the control of a strong promoter). Site directed mutagenesis was performed at position Arg340 (for mutations to Ala and Lys) and Asn213 to Ala. A clinical strain *A. baumannii* M9, the multidrug resistant (MDR) strain from which bla_{ADC} was initially cloned [8], was used as well.

For the ceftazidime/BATSI combinations, the substrate concentrations were varied while the inhibitors were tested at a constant concentration of 4 μg/mL according with the CLSI standards for β-lactamases inhibitors.

Protein Preparation and Purification

A construct containing amino acids D24-K383 of ADC-7, was expressed using a pET28a(+) plasmid and purified using a *m*-amino-phenylboronic acid resin (Sigma) as previously described.[10] The concentration of ADC-7 was calculated using the A_{280} with an

extinction coefficient of 46,300 M^{-1} cm^{-1} calculated for the expressed residues, D24-K383, by the ProtParam tool on the ExPASy bioinformatics portal.[31]

ADC-7 X-ray structure determination

ADC-7 crystals were grown at room temperature via hanging drop vapor diffusion using the following conditions: ADC-7 (3 mg/mL) in 25% w/v polyethylene glycol (PEG) 1500, 0.1 M succinate/phosphate/glycine buffer at pH 5.0 (SPG buffer, Molecular Dimensions). Crystals were harvested from the drop using a nylon loop and soaked for 2 hours in crystallization buffer containing 1 mM BATSI and subsequently cryocooled in liquid nitrogen. In the case of CR161, 1 mM of CR161 was included in the initial crystallization buffer and allowed to co-crystallize with ADC-7. Data were measured from an individual crystal at LS-CAT sector (21-1D-D and 21-1D-F beamlines) at the Advanced Photon Source at Argonne National Laboratory (Argonne, IL). Images were indexed, integrated and scaled with XDS.[32] Molecular replacement was completed with Phaser[33] using the ADC-7 apo structure from *Acinetobacter baumannii* (4U0T) with waters and ions removed.[10] Refinement was performed using Refmac5 in the CCP4 program suite.[32, 34] Repeated rounds of model building were completed in Coot.[35] The coordinates and structure parameters for the final ADC-7/BATSI complexes are available at the Protein Data Bank as **5WAC** (CR157), **5WAD** (CR161), **5WAE** (CR167), **5WAF** (CR192), and **5WAG** (S06017).

Steady State Kinetics

Competition kinetics were completed on a Cary 100 UV-vis spectrophotometer (Agilent Technologies). The K_i for the BATSIs was calculated by measuring the steady-state initial velocities in the presence of a constant concentration of 2 nM enzyme with increasing concentration of inhibitor against the colorimetric indicator substrate, 60 μM nitrocefin (NCF) in 10 mM phosphate-buffered saline (pH 7.4) as previously described.[12] In each assay, the

measurements were taken after a 5 minute pre-incubation of enzyme with BATSI. The average velocities (v_0) were then fitted to equation 1,

$$v_0 = v_u - \frac{v_u[I]}{K_{i(observed)}+[I]} \qquad (1)$$

where v_u represents the uninhibited turnover of NCF, $K_{i(observed)}$ is the concentration of inhibitor that results in a 50 percent reduction of v_u, and [I] is the concentration of inhibitor in the experiment. K_i values were also corrected for NCF affinity (K_m = 21.2 μM) according to equation 2,

$$K_{i(corrected)} = \frac{K_{i(observed)}}{1+\frac{[NCF]}{K_{mNCF}}} \qquad (2)$$

Circular Dichroism (CD)

Thermal denaturation and stability CD experiments were performed using a Jasco J-815 spectrometer (Easton, MD) with a Peltier effect temperature controller (GE Healthcare, Piscataway, NJ) as previously described.[10] Quartz cells with a 0.1 cm path length (Hellma, New York) were used for all experiments. Spectra were obtained with an ADC-7 concentration of 10 μM. Compounds were tested at a concentration of 50 μM to ensure that they do not interfere with the refraction of the light by the protein in the far UV spectrum. Thermal melting was performed between 20 and 80°C with a heating rate of 2°C/min. Raw equilibrium denaturation data, monitored by far-UV CD at 222 nm, were normalized to the fraction of denatured protein (f_u), and the data were used for calculations of melting temperature *Tm*. To determine if the thermal denaturation of ADC-7 follows a two-state process, the sample was monitored for changes in tertiary structure in the near-UV region, at 270 nm (data not shown), as previously described by

Beadle *et. al.* [36] The melting for near-UV CD was performed using 30 μg/mL ADC-7 and a heating rate of 2°C/min.

SUPPORTING INFORMATION

NMR spectra for the inhibitors

Abbreviations: ADC, *Acinetobacter*-derived Cephalosporinase; BLI, β-lactamase inhibitors; BATSI, boronic acid transition state inhibitor; NCF, nitrocefin; SSM, secondary structure matching; RMSD, root mean square deviation; MDR, multi-drug resistant; PDB, Protein Data Bank; NMR, nuclear magnetic resonance; MS, mass spectrometry.

AUTHOR INFORMATION

Corresponding authors: Brad Wallar, Ph.D., e-mail: wallarb@gvsu.edu, Phone: 616-331-3807; Rachel Powers, Ph.D., e-mail: powersra@gvsu.edu, Phone: 616-331-2853; Robert A. Bonomo, M.D., e-mail: robert.bonomo@va.gov; Phone: 216-791-3800 ext 4645

Author contributions: CR, EC, and FP synthesized all of the BATSI compounds. MAT and RAB performed microbiological assays, circular dichroism, and kinetics. RAP, BJW, AAB, HCS, KAS, and ALV performed kinetics and determined all of the crystal structures. All authors have contributed to the manuscript and have given approval to the final version of the manuscript.

ACKNOWLEDGMENTS

This work was supported in part by funds and/or facilities provided by the Cleveland Department of Veterans Affairs, the Department of Veterans Affairs Merit Review Program 1I01BX001974, the Veterans Integrated Service Network 10 Geriatric Research, Education, and Clinical Center (VISN 10 GRECC), and the National Institute of Allergy and Infectious Diseases of the National Institutes of Health under Award Number R01 AI072219, as well as National Institutes of Health R15 AI094489 (RAP). Use of the Advanced Photon Source, an Office of Science User Facility operated for the U.S. Department of Energy (DOE) Office of Science by Argonne National Laboratory, was supported by the U.S. DOE under Contract No. DE-AC02-06CH11357. Use of the LS-CAT Sector 21 was supported by the Michigan Economic Development Corporation and the Michigan Technology Tri-Corridor (Grant 085P1000817). Hollister Swanson (MaryBeth Koeze Fellow) and Alison VanDine were supported by the Student Summer Scholars Program in the Office of Undergraduate Research at GVSU.

Table 1A. Disc Susceptibility Assays (DSAs), in mm

	E.coli DH10B bla_{ADC-7}	*E.coli* DH10B $bla_{ADC-7,N213A}$	M9 clinical isolates
no antibiotic	6	6	6
CAZ – 10 μg	12	11	6
CAZ + 10 μg achiral cephalothin	17	16	8
CAZ + 10 μg S06017	15	15	6
CAZ + 10 μg CR167	22	18	12
CAZ + 10 μg CR157	24	17	15
CAZ + 10 μg CR161	26	20	16
CAZ + 10 μg CR192	20	15	14

Table 1B. MIC Values (μg/mL) in combination with 4 μg/mL BATSI compound.

Strain	CAZ	CAZ S06017	CAZ CR167	CAZ CR157	CAZ CR161	CAZ CR192	CAZ achiral cephalothin
E.coli DH10B	1	0.5	0.5	0.5	0.5	0.5	0.5
E.coli DH10B pBCSK, bla_{ADC-7}	64	16	1	1	0.5	2	32
E.coli DH10B pBCSK, $bla_{ADC-7, R340A}$	32	16	2	0.5	1	0.5	32
E.coli DH10B pBCSK, $bla_{ADC-7, R340K}$	32	16	4	1	1	2	32
E.coli DH10B pBCSK, $bla_{ADC-7, N213A}$	32	16	4	2	2	1	32
A. baumannii M9	>64	16	16	8	8	8	32

Table 2: Kinetic parameters and chemical structures for the various BATSIs. The variation in melting temperature T_m between T_m $^{ADC-7}$ = 61±1 °C and in complex with the boronic acid compounds shows an increase in the complex stability upon binding.

Compound	Chemical Structure	K_i [37]	Δ*Tm* [°C]
CR167	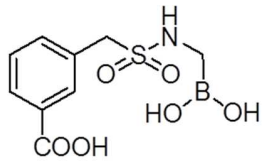	160	+ 2
CR157	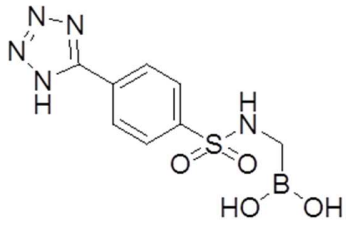	38	+ 4
CR161	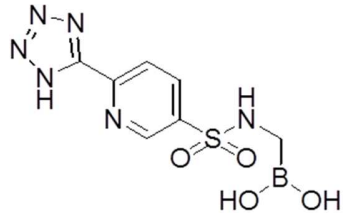	7.8	+ 5
CR192	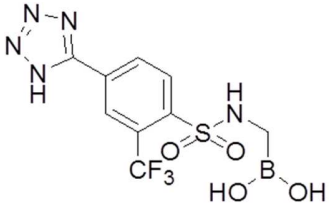	0.45	+ 9
S06017	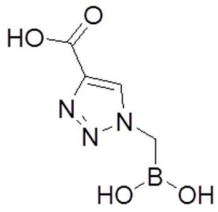	6,110	+ 2

Table 3. Crystallographic summary for the ADC-7/inhibitor complexes.

	ADC-7/CR167	ADC-7/CR157	ADC-7/CR161	ADC-7/CR192	ADC-7/S06017
Cell constants (Å; °)	a=88.79 b=81.05 c=105.06 β=113.45	a=88.35 b=80.67 c=104.98 β=113.42	a=89.27 b=81.47 c=105.91 β=112.50	a=89.02 b=81.28 c=106.38 β=112.64	a=88.67 b=80.90 c=105.34 β=113.36
Space group	$P2_1$	$P2_1$	$P2_1$	$P2_1$	$P2_1$
Resolution (Å)	1.80 (1.81-1.80)[a]	2.06 (2.07-2.06)[a]	2.09 (2.10-2.09)[a]	2.03 (2.04-2.03)[a]	1.93 (1.94-1.93)[a]
Unique reflections	124,952	82,849	82,578	90,002	99,952
Total observations	468,752	307,282	309,158	376,247	376,640
R_{merge} (%)	5.9 (66.2)	7.0 (55.3)	8.4 (66.6)	10.4 (65.2)	7.8 (63.2)
Completeness (%)[b]	99.4 (99.2)	98.9 (99.0)	99.3 (99.8)	99.5 (99.5)	97.4 (95.9)
$\langle I/\sigma_I \rangle$	15.1 (2.1)	11.6 (2.3)	11.5 (2.0)	8.8 (2.2)	10.8 (2.1)
Resolution range for refinement (Å)	50.00-1.80	48.17-2.06	50.00-2.09	50.00-2.03	50.00-1.93
Number of protein residues	1,422	1,418	1,406	1,422	1,424
Number of water molecules	586	188	370	349	389
RMSD bond lengths (Å)	0.019	0.015	0.015	0.016	0.017
RMSD bond angles (°)	1.952	1.745	1.790	1.832	1.864
R-factor (%)	18.3	20.3	21.4	21.5	18.6
R_{free} (%)[c]	23.2	26.4	28.6	27.7	24.7
Average B-factor, protein atoms ($Å^2$)	33.84	44.37	39.03	41.32	37.46
Average B-factor, inhibitor atoms ($Å^2$)	36.35	52.64	39.61	34.87	46.19
Average B-factor, water molecules ($Å^2$)	35.01	38.54	35.45	36.53	36.17

a. Values in parentheses are for the highest resolution shell.
b. Fraction of theoretically possible reflections observed.
c. R_{free} was calculated with 5% of reflections set aside randomly.

Figure 1: Structural differences between β-lactams, BLIs, and BATSIs. A. The cephalosporin, cephalothin, with the R1 and R2 side chains indicated. B. BLI, sulbactam. C. S02030 BATSI containing both R1 and R2 groups. D. CR192 BATSI containing only an R1. E. CR192 bound in tetrahedral molecular geometry to catalytic serine, with labeled O1 and O2 of the boronic acid.

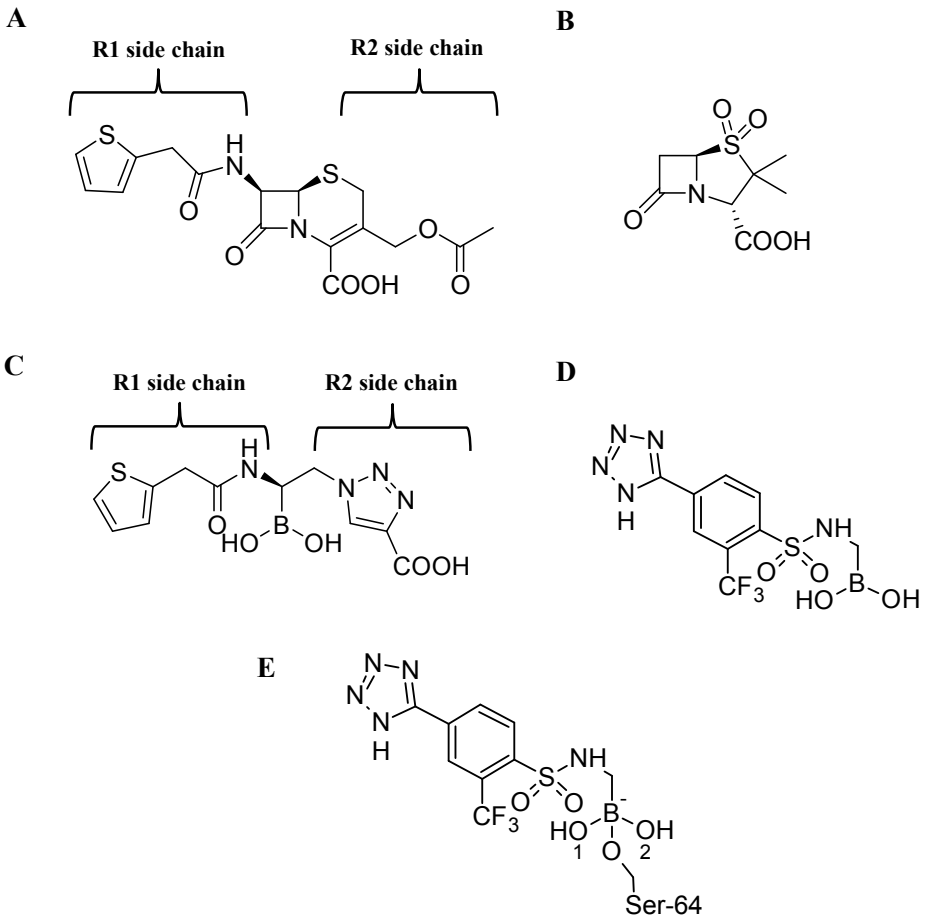

Figure 2. Thermal denaturation curves of ADC-7 enzyme and of the complexes between ADC-7 and boronic acid compounds. All compounds thermodynamically stabilize the enzyme. The largest variation of melting temperature *Tm* is observed for CR192. The compound stabilizes the enzyme from *Tm* ≈ 61 °C to almost 70 °C.

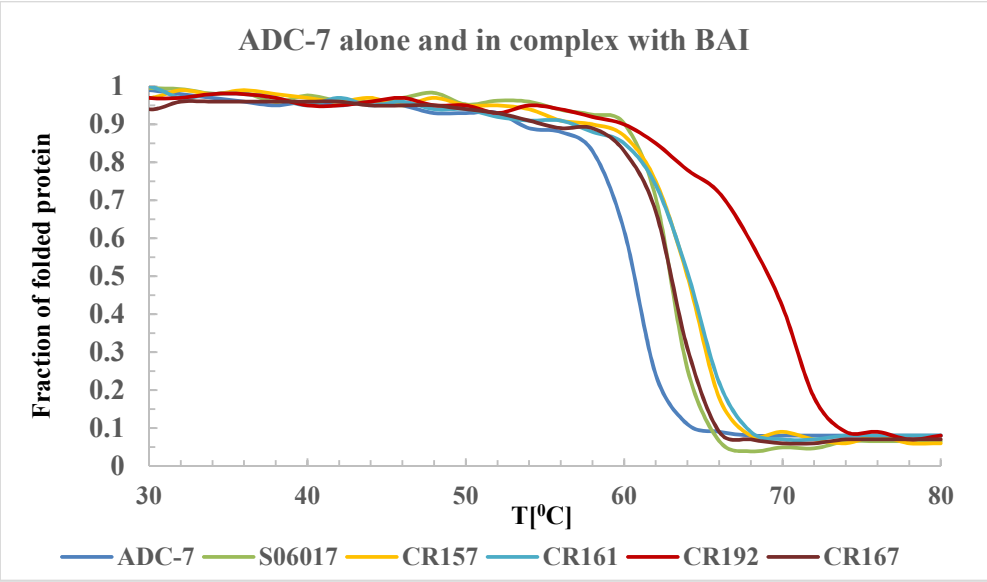

Figure 3: Stereoview of the various BATSIs covalently bound to catalytic Ser-64 with their respective electron density maps. F_o-F_c omit maps for the inhibitors, contoured at 3.0 σ, are displayed as a gray cage surrounding the model. A. CR157 (carbon atoms are colored green). B. CR161 (carbons white). C. CR167 (carbons magenta). D. CR192 (carbons cyan). E. S06017 (carbons gray). This and all subsequent figures are generated with PyMOL. [38]

A.

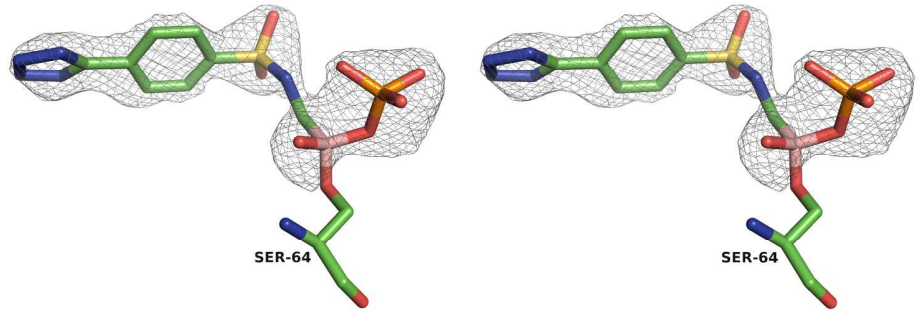

B.

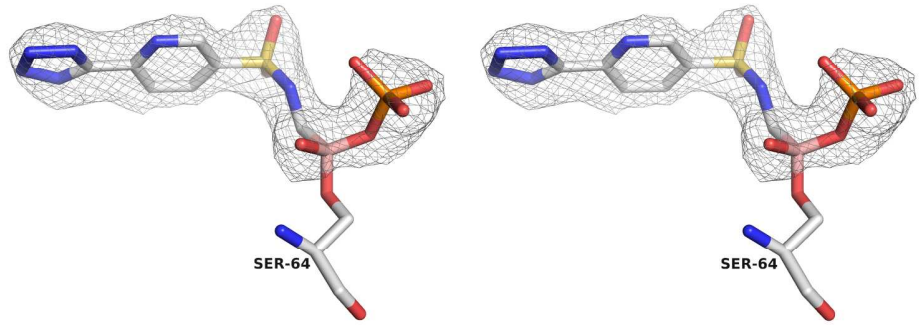

C.

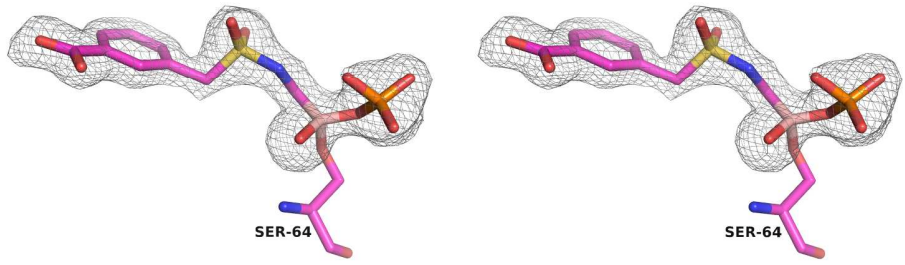

D.

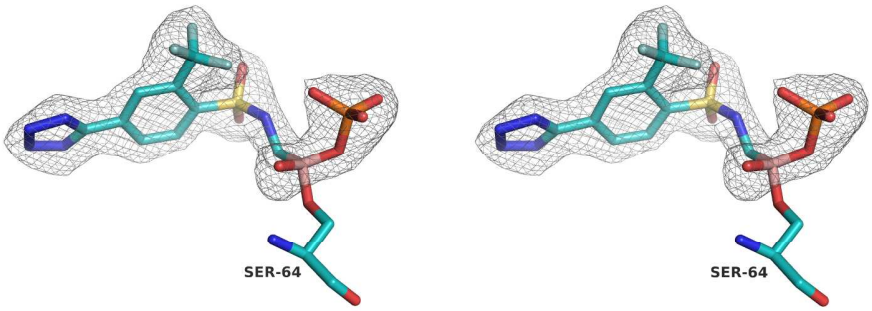

E.

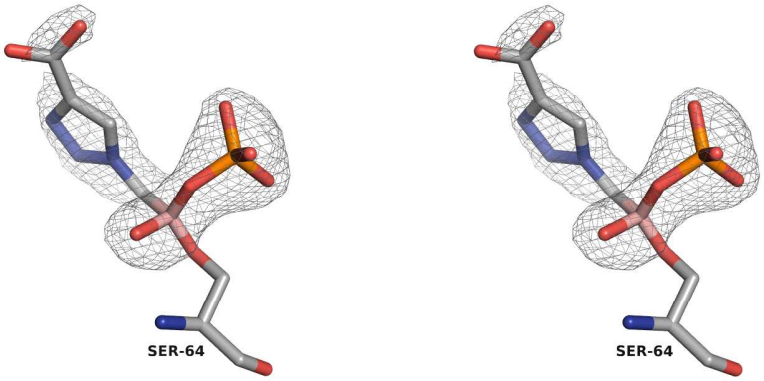

Figure 4: Stereoview of the ADC-7 active site in complex with various BATSIs. The carbon atoms of the active site residues and inhibitors are colored as followed. A. ADC-7/CR157 (green). B. ADC-7/CR161 (white). C. ADC-7/CR167 (magenta). D. ADC-7/CR192 (cyan). E. ADC-7/S06017 (gray). Hydrogen bonding interactions are shown as yellow dashed lines, and columbic interactions are shown as magenta dashed lines. Water molecules are shown as red spheres. Oxygens are colored red, nitrogens blue, boron pale pink, fluorines are white and phosphorous is colored orange.

A.

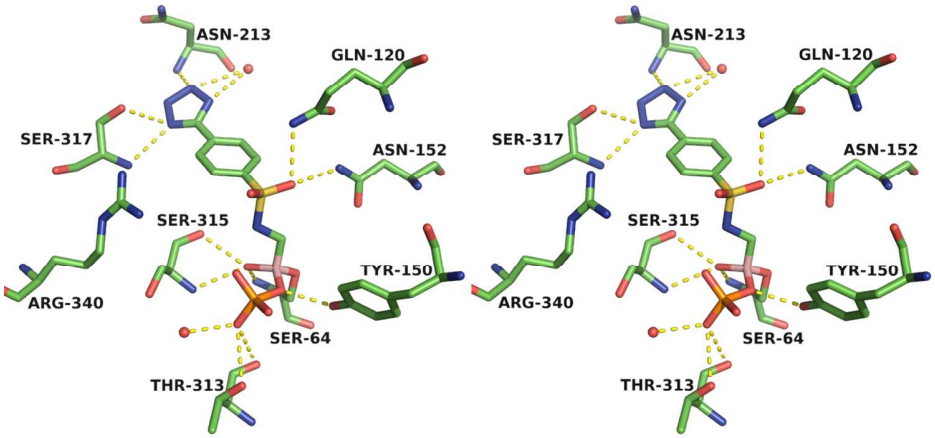

B.

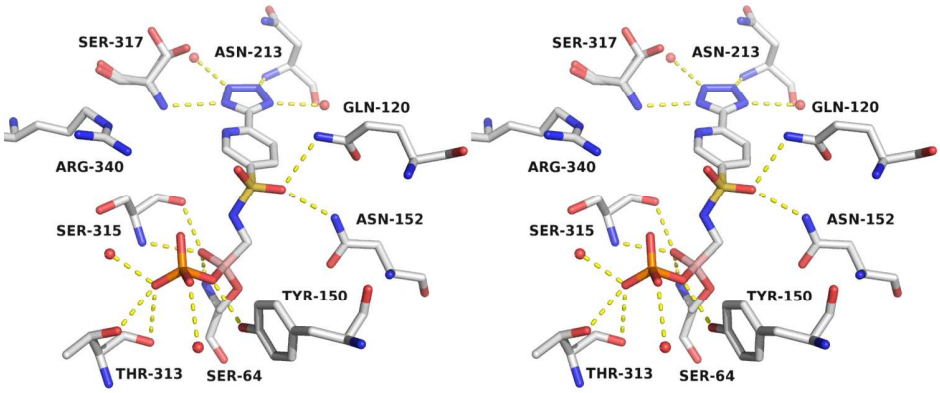

C.

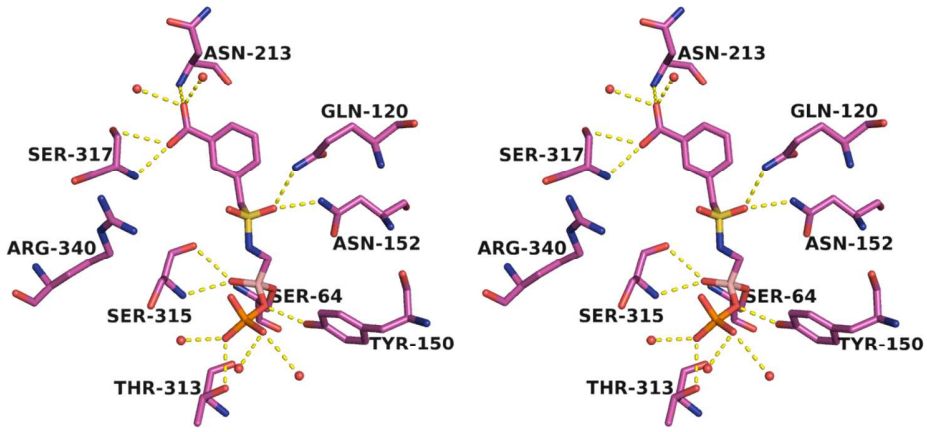
ASN-213
GLN-120
SER-317
ARG-340
ASN-152
SER-64
SER-315
TYR-150
THR-313
ASN-213
GLN-120
SER-317
ARG-340
ASN-152
SER-64
SER-315
TYR-150
THR-313

D.

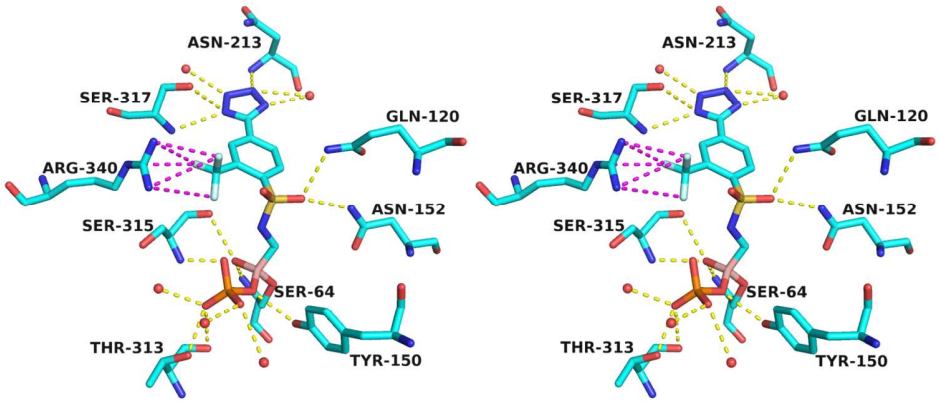
ASN-213
SER-317
GLN-120
ARG-340
ASN-152
SER-315
SER-64
THR-313
TYR-150
ASN-213
SER-317
GLN-120
ARG-340
ASN-152
SER-315
SER-64
THR-313
TYR-150

E.

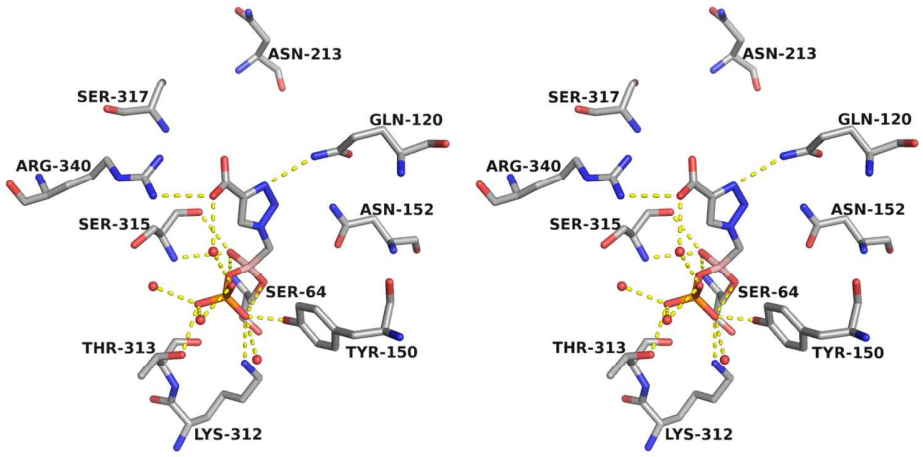
ASN-213
SER-317
GLN-120
ARG-340
ASN-152
SER-315
SER-64
THR-313
TYR-150
LYS-312
ASN-213
SER-317
GLN-120
ARG-340
ASN-152
SER-315
SER-64
THR-313
TYR-150
LYS-312

Figure 5: Superposition of ADC-7 in complex with three inhibitors: CR157 (green), CR161 (white), and CR192 (cyan).

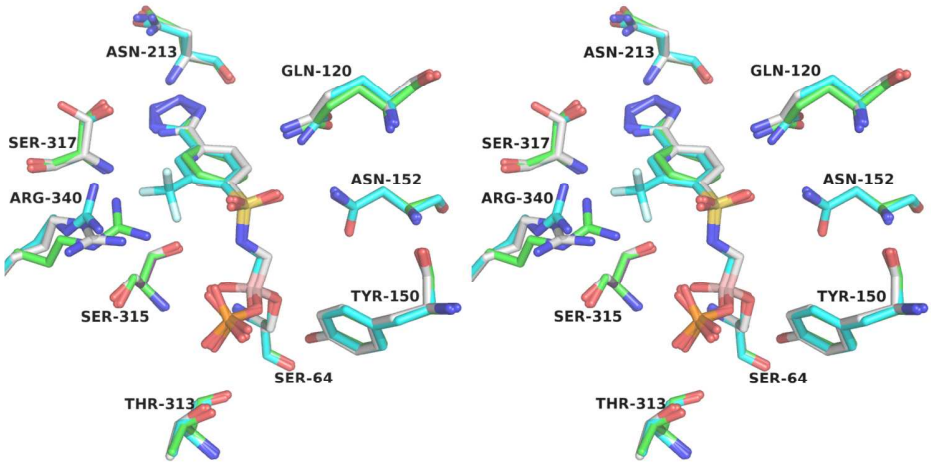

Figure 6: Stereoview of CR192 forming a potential columbic interaction between positively charged Arg340 and a net negative charge trifluoromethyl substituent.

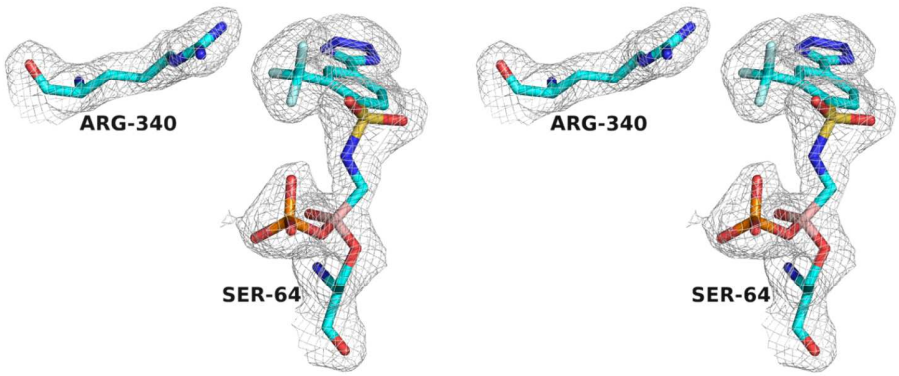

Figure 7: Interactions of Tyr222 with BATSIs. A. CR167 (magenta) forming parallel displaced π-π stacking with Tyr222 and B. CR157 (green) C. CR161 (white) D. CR192 (cyan) forming edge-to-face π-π stacking with Tyr 222.

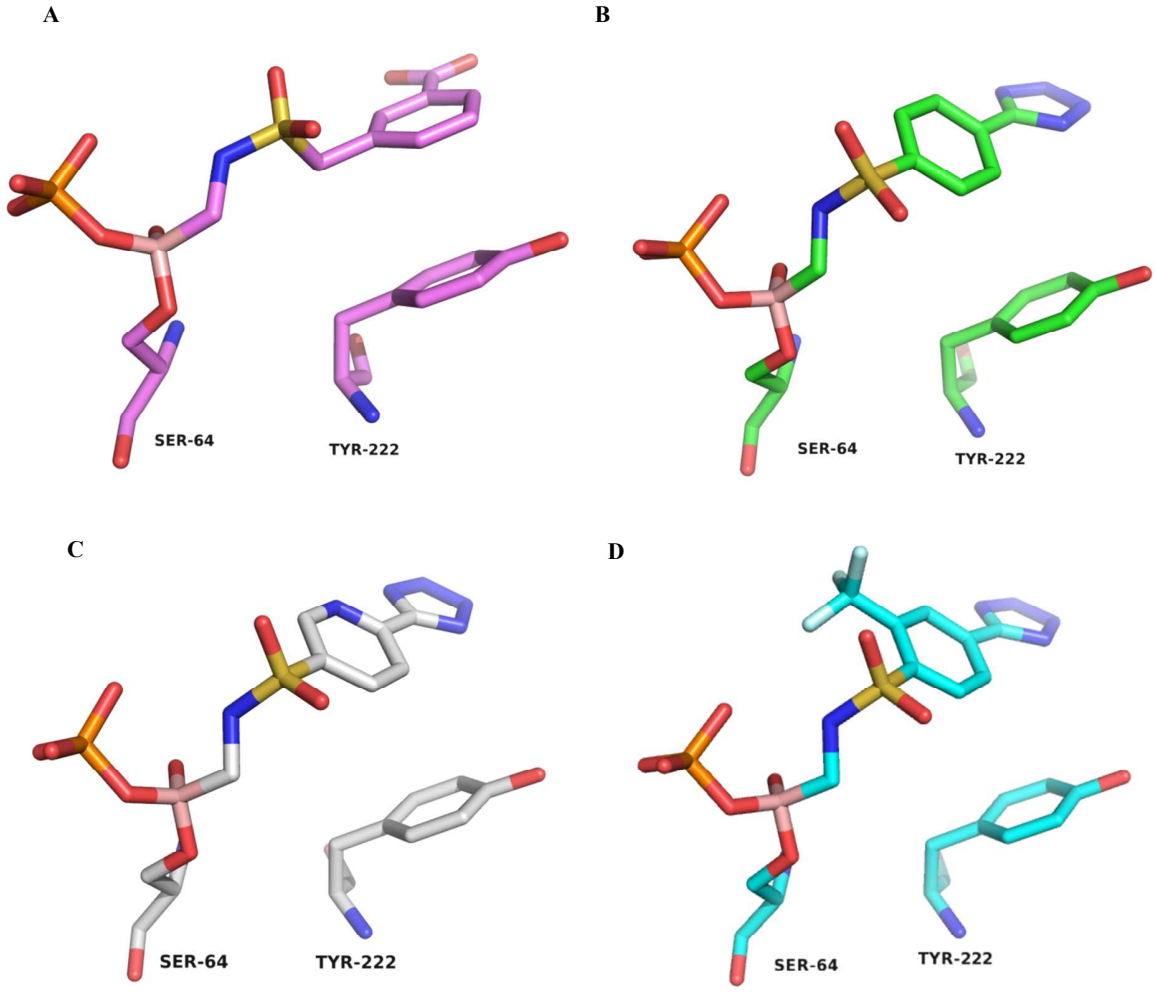

REFERENCES

1. Davies, J.; Davies, D., **(2010)** Origins and evolution of antibiotic resistance. *Microbiol Mol Biol Rev 74* (3), 417-33. DOI: 10.1128/MMBR.00016-10.
2. Bonomo, R. A.; Szabo, D., **(2006)** Mechanisms of multidrug resistance in *Acinetobacter* species and *Pseudomonas aeruginosa*. *Clin Infect Dis 43 Suppl 2*, S49-56. DOI: 10.1086/504477.
3. Perez, F.; Endimiani, A.; Bonomo, R. A., **(2008)** Why are we afraid of *Acinetobacter baumannii*? *Expert Rev Anti Infect Ther 6* (3), 269-71. DOI: 10.1586/14787210.6.3.269.
4. Perez, F.; Endimiani, A.; Ray, A. J.; Decker, B. K.; Wallace, C. J.; Hujer, K. M.; Ecker, D. J.; Adams, M. D.; Toltzis, P.; Dul, M. J.; Windau, A.; Bajaksouzian, S.; Jacobs, M. R.; Salata, R. A.; Bonomo, R. A., **(2010)** Carbapenem-resistant *Acinetobacter baumannii* and *Klebsiella pneumoniae* across a hospital system: impact of post-acute care facilities on dissemination. *J Antimicrob Chemother 65* (8), 1807-18. DOI: 10.1093/jac/dkq191.
5. Perez, F.; Hujer, A. M.; Hujer, K. M.; Decker, B. K.; Rather, P. N.; Bonomo, R. A., **(2007)** Global challenge of multidrug-resistant *Acinetobacter baumannii*. *Antimicrob Agents Chemother 51* (10), 3471-84. DOI: 10.1128/AAC.01464-06.
6. Wright, M. S.; Haft, D. H.; Harkins, D. M.; Perez, F.; Hujer, K. M.; Bajaksouzian, S.; Benard, M. F.; Jacobs, M. R.; Bonomo, R. A.; Adams, M. D., **(2014)** New insights into dissemination and variation of the health care-associated pathogen *Acinetobacter baumannii* from genomic analysis. *mBio 5* (1), e00963-13. DOI: 10.1128/mBio.00963-13.
7. Livermore, D. M., **(1998)** β-lactamase-mediated resistance and opportunities for its control. *J Antimicrob Chemother 41 Suppl D*, 25-41.
8. Hujer, K. M.; Hamza, N. S.; Hujer, A. M.; Perez, F.; Helfand, M. S.; Bethel, C. R.; Thomson, J. M.; Anderson, V. E.; Barlow, M.; Rice, L. B.; Tenover, F. C.; Bonomo, R. A., **(2005)** Identification of a new allelic variant of the *Acinetobacter baumannii* cephalosporinase, ADC-7 β-lactamase: defining a unique family of class C enzymes. *Antimicrob Agents Chemother 49* (7), 2941-8. DOI: 10.1128/AAC.49.7.2941-2948.2005.
9. Tian, G. B.; Adams-Haduch, J. M.; Taracila, M.; Bonomo, R. A.; Wang, H. N.; Doi, Y., **(2011)** Extended-spectrum AmpC cephalosporinase in *Acinetobacter baumannii*: ADC-56 confers resistance to cefepime. *Antimicrob Agents Chemother 55* (10), 4922-5. DOI: 10.1128/AAC.00704-11.
10. Powers, R. A.; Swanson, H. C.; Taracila, M. A.; Florek, N. W.; Romagnoli, C.; Caselli, E.; Prati, F.; Bonomo, R. A.; Wallar, B. J., **(2014)** Biochemical and structural analysis of inhibitors targeting the ADC-7 cephalosporinase of *Acinetobacter baumannii*. *Biochemistry 53* (48), 7670-9. DOI: 10.1021/bi500887n.
11. Drawz, S. M.; Bonomo, R. A., **(2010)** Three decades of β-lactamase inhibitors. *Clin Microbiol Rev 23* (1), 160-201. DOI: 10.1128/CMR.00037-09.
12. Crompton, I. E.; Cuthbert, B. K.; Lowe, G.; Waley, S. G., **(1988)** β-lactamase inhibitors. The inhibition of serine β-lactamases by specific boronic acids. *Biochem. J. 251* (2), 453-459.
13. Bou, G.; Santillana, E.; Sheri, A.; Beceiro, A.; Sampson, J. M.; Kalp, M.; Bethel, C. R.; Distler, A. M.; Drawz, S. M.; Pagadala, S. R.; van den Akker, F.; Bonomo, R. A.; Romero, A.; Buynak, J. D., **(2010)** Design, synthesis, and crystal structures of 6-

alkylidene-2'-substituted penicillanic acid sulfones as potent inhibitors of *Acinetobacter baumannii* OXA-24 carbapenemase. *J Am Chem Soc 132* (38), 13320-31. DOI: 10.1021/ja104092z.

14. Pratt, R. F., **(1989)** Inhibition of a class C β-lactamase by a specific phosphonate monoester. *Science 246* (4932), 917-9.
15. Wyrembak, P. N.; Babaoglu, K.; Pelto, R. B.; Shoichet, B. K.; Pratt, R. F., **(2007)** O-aryloxycarbonyl hydroxamates: new β-lactamase inhibitors that cross-link the active site. *J Am Chem Soc 129* (31), 9548-9. DOI: 10.1021/ja072370u.
16. Coleman, K., **(2011)** Diazabicyclooctanes (DBOs): a potent new class of non-β-lactam β-lactamase inhibitors. *Curr Opin Microbiol 14* (5), 550-5. DOI: 10.1016/j.mib.2011.07.026.
17. King, A. M.; King, D. T.; French, S.; Brouillette, E.; Asli, A.; Alexander, J. A.; Vuckovic, M.; Maiti, S. N.; Parr, T. R., Jr.; Brown, E. D.; Malouin, F.; Strynadka, N. C.; Wright, G. D., **(2016)** Structural and Kinetic Characterization of Diazabicyclooctanes as Dual Inhibitors of Both Serine-β-Lactamases and Penicillin-Binding Proteins. *ACS Chem Biol 11* (4), 864-8. DOI: 10.1021/acschembio.5b00944.
18. Mosley, J. F., 2nd; Smith, L. L.; Parke, C. K.; Brown, J. A.; Wilson, A. L.; Gibbs, L. V., **(2016)** Ceftazidime-Avibactam (Avycaz): For the Treatment of Complicated Intra-Abdominal and Urinary Tract Infections. *P T 41* (8), 479-83.
19. Eidam, O.; Romagnoli, C.; Dalmasso, G.; Barelier, S.; Caselli, E.; Bonnet, R.; Shoichet, B. K.; Prati, F., **(2012)** Fragment-guided design of subnanomolar β-lactamase inhibitors active in vivo. *Proc Natl Acad Sci U S A 109* (43), 17448-53. DOI: 10.1073/pnas.1208337109.
20. Morandi, S.; Morandi, F.; Caselli, E.; Shoichet, B. K.; Prati, F., **(2008)** Structure-based optimization of cephalothin-analogue boronic acids as β-lactamase inhibitors. *Bioorganic & medicinal chemistry 16* (3), 1195-205. DOI: 10.1016/j.bmc.2007.10.075.
21. Beadle, B. M.; Trehan, I.; Focia, P. J.; Shoichet, B. K., **(2002)** Structural milestones in the reaction pathway of an amide hydrolase: substrate, acyl, and product complexes of cephalothin with AmpC β-lactamase. *Structure 10* (3), 413-24.
22. Romagnoli, C.; Caselli, E.; Prati, F., **(2015)** Synthesis of 1,2,3-triazol-1-yl-methaneboronic acids via click chemistry: an easy access to a new potential scaffold for protease inhibitors. *European J Org Chem 2015* (5), 1075-1083. DOI: 10.1002/ejoc.201403408.
23. Chaudhari, S. R.; Mogurampelly, S.; Suryaprakash, N., **(2013)** Engagement of CF3 group in N-H...F-C hydrogen bond in the solution state: NMR spectroscopy and MD simulation studies. *J Phys Chem B 117* (4), 1123-9. DOI: 10.1021/jp310798d.
24. Murray, J. S.; Lane, P.; Politzer, P., **(2009)** Expansion of the sigma-hole concept. *Journal of molecular modeling 15* (6), 723-9. DOI: 10.1007/s00894-008-0386-9.
25. Wang, C.; Guan, L.; Danovich, D.; Shaik, S.; Mo, Y., **(2016)** The origins of the directionality of noncovalent intermolecular interactions. *J Comput Chem 37* (1), 34-45. DOI: 10.1002/jcc.23946.
26. Sirimulla, S.; Bailey, J. B.; Vegesna, R.; Narayan, M., **(2013)** Halogen interactions in protein-ligand complexes: implications of halogen bonding for rational drug design. *J Chem Inf Model 53* (11), 2781-91. DOI: 10.1021/ci400257k.

27. Egli, M.; Tereshko, V.; Mushudov, G. N.; Sanishvili, R.; Liu, X.; Lewis, F. D., **(2003)** Face-to-face and edge-to-face pi-pi interactions in a synthetic DNA hairpin with a stilbenediether linker. *J Am Chem Soc 125* (36), 10842-9. DOI: 10.1021/ja0355527.
28. McGaughey, G. B.; Gagne, M.; Rappe, A. K., **(1998)** pi-Stacking interactions. Alive and well in proteins. *J. Biol. Chem. 273* (25), 15458-15463.
29. Hohenstein, E. G.; Sherrill, C. D., **(2009)** Effects of heteroatoms on aromatic pi-pi interactions: benzene-pyridine and pyridine dimer. *J Phys Chem A 113* (5), 878-86. DOI: 10.1021/jp809062x.
30. Institute, C. a. L. S., **(2007)** Performance Standards for Antimicrobial Susceptibility Testing; Seventeenth Informational Supplement. *27* (M100-S17).
31. Perichon, B.; Goussard, S.; Walewski, V.; Krizova, L.; Cerqueira, G.; Murphy, C.; Feldgarden, M.; Wortman, J.; Clermont, D.; Nemec, A.; Courvalin, P., **(2014)** Identification of 50 class D β-lactamases and 65 *Acinetobacter*-derived cephalosporinases in *Acinetobacter* spp. *Antimicrob Agents Chemother 58* (2), 936-49. DOI: 10.1128/AAC.01261-13.
32. Murshudov, G. N.; Vagin, A. A.; Dodson, E. J., **(1997)** Refinement of macromolecular structures by the maximum-likelihood method. *Acta Crystallogr D Biol Crystallogr 53* (Pt 3), 240-55.
33. McCoy, A. J.; Grosse-Kunstleve, R. W.; Adams, P. D.; Winn, M. D.; Storoni, L. C.; Read, R. J., **(2007)** Phaser crystallographic software. *J Appl Crystallogr 40* (Pt 4), 658-674.
34. CCP4 (Collaborative Computational Project Number 4), **(1994)** The CCP4 suite: programs for protein crystallography. *Acta Crystallographica Section D 50* (5), 760-763. DOI: doi:10.1107/S0907444994003112.
35. Emsley, P.; Cowtan, K., **(2004)** Coot: Model-building tools for molecular graphics. *Acta Crystallogr D 60*, 2126-2132.
36. Beadle, B. M.; McGovern, S. L.; Patera, A.; Shoichet, B. K., **(1999)** Functional analyses of AmpC β-lactamase through differential stability. *Protein Sci. 8* (9), 1816-1824.
37. Hajduk, P. J.; Sheppard, G.; Nettesheim, D. G.; Olejniczak, E. T.; Shuker, S. B.; Meadows, R. P.; Steinman, D. H.; Carrera, G. M.; Marcotte, P. A.; Severin, J.; Walter, K.; Smith, H.; Gubbins, E.; Simmer, R.; Holzman, T. F.; Morgan, D. W.; Davidsen, S. K.; Summers, J. B.; Fesik, S. W., **(1997)** Discovery of potent nonpeptide inhibitors of stromelysin using SAR by NMR. *J. Am. Chem. Soc. 119* (25), 5818-5827.
38. *The PyMOL Molecular Graphics System, Version 1.3, Schrödinger, LLC.*

FOR TABLE OF CONTENTS USE ONLY